Nanostructural Perspective for Destabilization of Mg Hydride Using the Immiscible Transition Metal Mn

Lu, Yanshan; Asano, Kohta; Schreuders, Herman; Kim, Hyunjeong; Sakaki, Kouji; Machida, Akihiko; Watanuki, Tetsu; Dam, Bernard

DOI
10.1021/acs.inorgchem.1c02525

Publication date
2021

Document Version
Final published version

Published in
Inorganic Chemistry

Inorganic Chemistry

pubs.acs.org/IC Article

Nanostructural Perspective for Destabilization of Mg Hydride Using the Immiscible Transition Metal Mn

Yanshan Lu, Kohta Asano,* Herman Schreuders, Hyunjeong Kim, Kouji Sakaki, Akihiko Machida, Tetsu Watanuki, and Bernard Dam

Cite This: *Inorg. Chem.* 2021, 60, 15024−15030 Read Online

ACCESS | Metrics & More | Article Recommendations | Supporting Information

ABSTRACT: Phase segregation in hydride-forming alloys may persist under the action of multiple hydrogenation/dehydrogenation cycles. We use this effect to destabilize metal hydrides in the immiscible Mg−Mn system. Here, in the Mg_xMn_{1-x} thin films, the Mg and Mn domains are chemically segregated at the nanoscale. In Mn-rich compositions, the desorption pressure of hydrogen from MgH_2 is elevated at a given temperature, indicating a thermodynamic destabilization. The increase in the desorption pressure of hydrogen reaches ~2.5 orders in magnitude for $x = 0.30$ at moderate temperatures. Such large thermodynamic destabilization allows the MgH_2 to reversibly absorb and desorb hydrogen even at room temperature. Our strategy to use immiscible elements for destabilization of MgH_2 is effective and opens up the possibility for the development of advanced and low-cost hydrogen storage and supply systems.

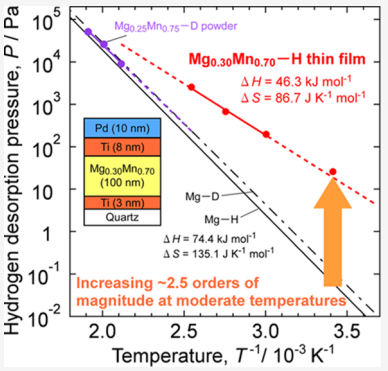

INTRODUCTION

Hydrogen is one of the promising energy carriers in a global sustainable society because it can be produced by electrolyzing water using renewable energy generation.[1] Recently, it has been shown that hydrocarbons such as methane can be produced from hydrogen and carbon dioxide, to establish efficient carbon recycling.[2,3] In the next decade or two, safe and compact storage and supply technologies of hydrogen will be necessary, not only in industrial areas but also in urban areas. Metal hydrides can store hydrogen at moderate pressures, in which the volumetric density of hydrogen is higher than gaseous storage compressed up to 70 MPa.[4,5] Mg is one of the most attractive metals because of its lightweight and low material costs. However, hydride-phase MgH_2 is too stable to release hydrogen at moderate temperatures, and thus, thermodynamic destabilization is essential for practical applications.

Theoretical calculations have indicated that MgH_2 thin layers with a thickness below 10 unit cells[6] and MgH_2 particles with a grain size smaller than 1.3 nm[7] would reduce the stability of MgH_2. Alterations in hydrogen absorption/desorption properties were reported in Mg and its alloy thin films prepared by means of magnetron sputtering.[8−10] It has been shown that in addition to nanosizing, the utilization of immiscible metals with Mg can modify the thermodynamics more effectively.[11−14] A multilayer stack of Mg/Ti with a typical layer thickness below 10 nm revealed a large destabilization of MgH_2 due to the extra contribution of the interface energy difference $\Delta\gamma$ between Mg/TiH_2 and MgH_2/TiH_2.[15] For Ti-rich Mg−Ti alloy thin films and powders, nanometer-sized MgH_2 clusters coherently embedded in a TiH_2 matrix are formed upon hydrogenation, again resulting in enhanced destabilization of MgH_2 by the interface energy.[16,17] Recently, we succeeded in obtaining an even more destabilized MgH_2 by the addition of Cr to the Mg−Ti system: Cr is also immiscible with Mg and expected to increase the interface energy effect.[18]

Destabilization of MgH_2 was also observed in Ti-free immiscible Mg−Mn and Mg−Cr powders prepared by ball milling.[19,20] These alloy powders reversibly absorb and desorb hydrogen at a relatively low temperature of 473 K without adding any catalysts. This improvement was attributed to lattice distortion induced by nanosizing MgH_2 and in part also to the interface energy effect. Synthesizing other immiscible Mg−X (X: Zr, V, etc.) alloys and their hydrogenation/dehydrogenation properties have also been reported.[21−26] Among the immiscible Mg systems, Mg−Mn alloys are attractive because of the low material costs. However, the enthalpy for deuteride dissociation of the $Mg_{0.25}Mn_{0.75}$−D powder was found to be $\Delta H = 71.5$ kJ mol^{-1}−D_2, not much different from the value $\Delta H = 73.1$ kJ mol^{-1}−D_2 ($\Delta H = 74.4$ kJ mol^{-1}−H_2) found for conventional bulk Mg−D(H).[27] To investigate this system in more detail, we need model samples,

Received: August 16, 2021
Published: September 20, 2021

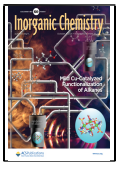

https://doi.org/10.1021/acs.inorgchem.1c02525
Inorg. Chem. 2021, 60, 15024−15030

in which very fine Mg and Mn domains are well mixed. Ultimately, we hope to be able to forecast more destabilized MgH_2 combining immiscible low-cost metals.

In the present work, we synthesize Mg−Mn thin films by means of magnetron cosputtering and evaluate the hydrogenation and dehydrogenation behaviors. The optical transmission change in the thin film occurs during the hydrogen absorption/desorption, corresponding to the transformation between the metallic Mg and transparent MgH_2 phases. The stability of the MgH_2 phase is evaluated by measuring the pressure P−optical transmission T isotherms. This method is called "hydrogenography".[28,29] We measured the isotherms of the thin films at specific temperatures including room temperature, where the hydrogen absorption/desorption of bulk/powder samples hardly proceeds. We will discuss the optimal nanostructure suitable for the destabilization and cyclic durability, together with the perspective to tune the stability of MgH_2 using the immiscible metals.

EXPERIMENTAL SECTION

Synthesis of Immiscible Mg−Mn Thin Films. Mg/Mn multilayer stacks and Mg_xMn_{1-x} alloy thin films were deposited at room temperature on quartz, glass, and Kapton substrates under an argon pressure (purity 6 N) of 0.8 Pa in an ultrahigh vacuum RF/DC magnetron cosputtering system (base pressure 10^{-7} Pa) with off-centered sources (AVC, ASE-4SA). The Mg/Mn multilayer stack is composed of 10 nm-thick Mn layers and three Mg layers with a thickness of 2, 5, and 10 nm. For the Mg_xMn_{1-x} ($0 \le x \le 0.75$) alloy thin films, to measure the P−T isotherms, the alloy layer with a thickness of 100 nm is deposited on the substrate with 3 and 8 nm adhesive Ti layers. Finally, a Pd capping layer with a thickness of 10 nm was deposited on the top to prevent oxidation and promote hydrogenation.

Hydrogenography. The P−T isotherms of our multilayer stacks and alloy thin films were evaluated by means of hydrogenography.[28,29] Before the measurements, the alloy thin films were precycled with hydrogen absorption and desorption at room temperature to obtain a reproducible optical response. According to the Lambert−Beer law, the relation $\ln(T/T_0)$ is proportional to $C_H d$, where T_0 is the initial transmission, C_H is the hydrogen content in the film, and d is the film thickness.[28,29] Pure H_2, Ar-3.91% H_2, and Ar-0.097% H_2 gases were properly used depending on the pressure range of hydrogen.

Characterization. X-ray diffraction (XRD) of Mg_xMn_{1-x} ($0 \le x \le 0.64$) thin films with a thickness of 200 nm covered with a uniform 5 nm layer of Pd, which were deposited on glass substrates, was measured using a Rigaku 2500V diffractometer with Cu Kα radiation and a θ−2θ goniometer. Synchrotron X-ray diffraction experiments were carried out at the BL22XU beamline at SPring-8.[30] For this experiment, we deposited Mg_xMn_{1-x} ($0.50 \le x \le 0.75$) alloy thin films with a thickness of 400 nm covered with a uniform 3 nm layer of Pd on both sides of a 7.5 μm-thick Kapton substrate, then cut the films into small pieces, and packed them in a Kapton capillary with an outer diameter of 1 mm.[31] The Kapton capillaries were spun for ±30° during data collection. All the data of the thin films were collected at room temperature using an amorphous silicon detector manufactured by PerkinElmer. The X-ray energy was 69.717 keV (λ = 0.17783 Å).

RESULTS AND DISCUSSION

Hydrogenation and Dehydrogenation Behavior of Mg−Mn Thin Films. First, we consider a Mg/Mn multilayer stack consisting of three Mg layers with a thickness of 2, 5, and 10 nm separated by 10 nm layers of Mn. Figure 1 shows the P−T isotherm of the multilayer stack measured under the hydrogen pressure of up to 10^5 Pa at 293 K during the first hydrogen absorption process. Under the applied conditions, it is difficult for Mn to form a hydride phase.[32] Although Pd

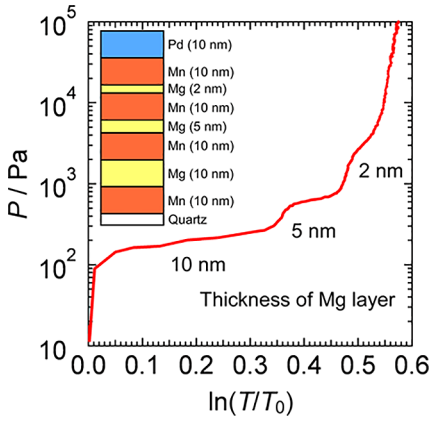

Figure 1. Schematic representation of the Mg/Mn multilayer geometry and P−T isotherm measured at 293 K during the first hydrogen absorption process where the transition from Mg to MgH_2 takes place as a function of the thicknesses of 2, 5, and 10 nm.

should form a hydride phase at $P \approx 6 \times 10^2$ Pa at this temperature,[33] PdH_x remains metallic, and thus, the optical change upon hydrogenation is much smaller than that of Mg.[28,29] Hence, the optical change of $\ln(T/T_0)$ is mainly due to the hydrogenation of the Mg layers. Clearly, we observe three steps in the plateau region, which are attributed to the coexistence of the metallic Mg and transparent MgH_2 phases. The previous studies have shown that the plateau pressure increases with decreasing Mg thickness, and the width of the plateau increases with the thickness/volume of the material,[11,15,18] while the elevating effect of the plateau pressure by facing with immiscible metals (Ti, V, and Nb) is smaller than that with miscible ones (Ni and Pd).[11] Accordingly, the widest plateau at $P \approx 2 \times 10^2$ Pa originates from the 10 nm layer of Mg, which loads hydrogen first. The narrower plateaus at $P \approx 7 \times 10^2$ and 3×10^3 Pa correspond to the hydrogenation of the 5 and 2 nm layers of Mg, respectively. This result suggests the possibility to alter the thermodynamics of nanometer-sized MgH_2 by facing it with immiscible Mn, which is a nonhydride-forming element. The immiscibility of the Mg/Mn two-dimensional stack may lead to quasi-free interfaces,[11] differing from three-dimensional embedding. The lattice expansion during hydrogenation requires plastic deformation, which raises the plateau pressure.[15] Similarly, the desorption plateau pressure may be lowered due to plastic deformation, although the interface energy effect contributes to an increase in the plateau pressure,[15] but this could not be observed due to the lower limit of the pressure gauge.

Considering that the desorption thermodynamics of MgH_2 was observed to be altered in Mg−Mn−H powders,[19,20] we next evaluated the hydrogenation and dehydrogenation behaviors of Mg−Mn *alloy* thin films. Although the alloy layer is sandwiched with two adhesive Ti layers, the optical effect of the hydrogenation of Ti is negligible under the applied conditions because Ti forms a stable hydride phase under much lower pressure of hydrogen than that of Mg.[32] All Mg_xMn_{1-x} alloy thin films were precycled at room temperature before the measurements of the P−T isotherms. As a result, we obtained reproducible optical responses at least up to the 10th cycle (Figure S1a,b). This is probably because the immiscibility of Mg/Mn does not allow stable alloy phases. In Figure 2, we show the P−T isotherms for Mg_xMn_{1-x}−H_2 (x = 0.30, 0.50, 0.60, and 0.75) systems at 293 K. We observe that the optical

https://doi.org/10.1021/acs.inorgchem.1c02525
Inorg. Chem. 2021, 60, 15024−15030

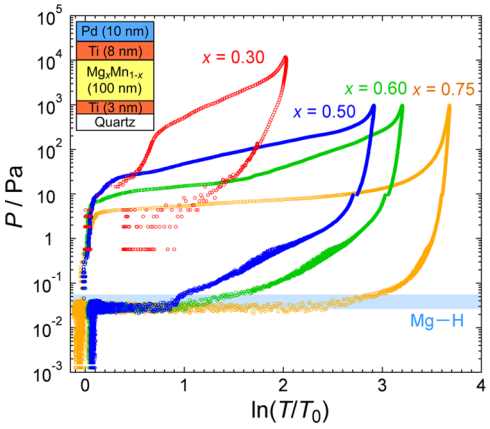

Figure 2. $P-T$ isotherms of the $Mg_xMn_{1-x}-H_2$ (x = 0.30, 0.50, 0.60, and 0.75) system at 293 K where the transition between Mg and MgH_2 as a function of the Mg content is evidenced by a change in transmission. The resolution of the desorption process below ~10 Pa for x = 0.30 is low due to the limited significant digits of the pressure gauge. The small gap at 10 Pa for x = 0.50, 0.60, and 0.75 is due to switching the measurement range of the pressure gauge. The light-blue line indicates the dehydrogenation pressure of bulk MgH_2 calculated from the extrapolation of the Van't Hoff plot.[27]

contrast—which is due to the transformation between the metallic Mg and transparent MgH_2 phases—increases with increasing Mg content/fraction x. The absorption pressure increases with decreasing Mg content and reaches values of 10^3 Pa for x = 0.30. In this case, we do observe the dehydrogenation plateau, and the equilibrium hydrogen pressure for hydrogenation is 2−3 orders of magnitude higher than that for dehydrogenation. The out-of-plane expansion upon hydrogenation of the thin film induces high plastic deformation energy even after hydrogenation/dehydrogenation precycles, which leads to a larger hysteresis than bulk materials.[15,34]

Let us then focus on the desorption process. For x = 0.30, the plateau region exhibits a steep slope, and the resolution below $P \approx 5$ Pa $[\ln(T/T_0) \approx 1]$ is low due to the limited significant digits of the pressure gauge. The sloping plateaus show higher hydrogen desorption pressure than that of bulk MgH_2, which is calculated from the extrapolation of the Van't Hoff plot[27] and shown by a light-blue line. Possibly, this is due to a range of Mg domain sizes. In our previous study, in the Ti-rich Mg_xTi_{1-x}−H thin films, we found that the Mg domains have a size distribution with the minimum size estimated to be ~2 nm.[16] Small MgH_2 domains were more effectively destabilized, resulting in the higher plateau pressure.

We suggest that the size of the Mg domains is related to the volume fraction of Mg. Similar to the Mg_xTi_{1-x},[16] we estimate the trend of the volume fraction of Mg, V_{Mg}, from the atomic weight and density of Mg and Mn, simply assuming that Mg and Mn domains are segregated in Mg_xMn_{1-x} and that the volume of their boundaries is ignored (Figure 3). The V_{Mg} increases with increasing Mg content x and reaches 0.5 at $x \approx$ 0.35. This indicates that Mg becomes the minority volume fraction below $x \approx 0.35$ and may tend to form domains, which are embedded in a Mn matrix. This may explain the remarkable increase in the desorption pressure of the $P-T$ isotherm at x = 0.30. For x = 0.50 and 0.60, a part of the Mg is no longer present in the form of destabilized MgH_2. In particular, the desorption pressure at x = 0.75 is largely

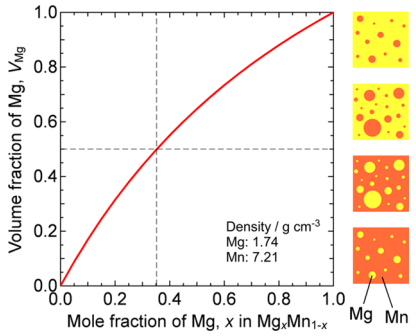

Figure 3. Calculated volumetric fraction of Mg V_{Mg} in Mg_xMn_{1-x} and schematic image of distribution of Mg and Mn domains.

equivalent to that of bulk Mg as the light-blue line. More details of the metallographic structure will be discussed in the next section.

Note that in Mg_xTi_{1-x}−H thin films, the sloping desorption plateau of the $P-T$ isotherm was partially lower than the desorption pressure of bulk MgH_2.[16] This stabilization of a part of MgH_2 was due to local dissolution of Ti into the Mg domains, where hydrogen occupying the interstitial sites is stabilized by the Ti coordination since Ti forms more stable hydride phases than Mg. The advantage of the nanostructure consisting of Mg and Mn is a nonhydride-forming matrix of Mn, leading only to the destabilization effect of MgH_2 without any interfering stabilization effect.

Nanostructure to Generate Destabilization of MgH_2 in Mg_xMn_{1-x}(−H) Thin Films. To characterize destabilized MgH_2 in Mg_xMn_{1-x}(−H) thin films, we measured XRD patterns of as-deposited and hydrogenated thin films deposited on a glass substrate (Figure 4). For the Mn (x = 0) film

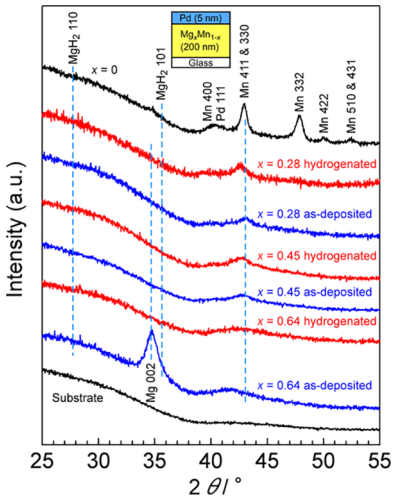

Figure 4. X-ray diffraction patterns of as-deposited and hydrogenated Mg_xMn_{1-x} (x = 0.28, 0.45, and 0.64) and Mn (x = 0) thin films capped with a Pd layer and a glass substrate.

covered by 5 nm of Pd, diffraction peaks of α-Mn (space group: $I\bar{4}3m$) are observed. This result indicates that the Mn layer is polycrystalline and does not have a high preferred orientation. It is well known that metal thin films with a high symmetry structure often have a single growth direction, for example, ⟨111⟩ of fcc Pd and ⟨001⟩ of hcp Mg and Ti.[15,16] However, the α-Mn thin film does not show a strong texture under the present deposition conditions probably because of a

https://doi.org/10.1021/acs.inorgchem.1c02525
Inorg. Chem. 2021, 60, 15024−15030

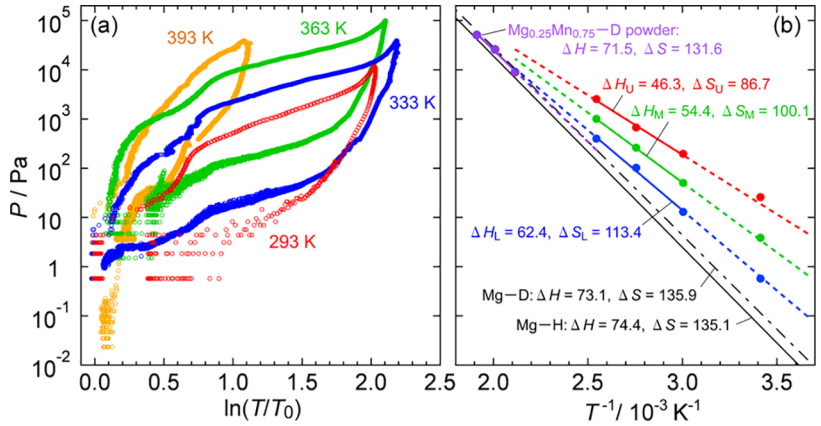

Figure 5. (a) $P-T$ isotherms (T: optical transmission) and (b) Van't Hoff plots of the $Mg_{0.30}Mn_{0.70}-H_2$ system at 293, 333, 363, and 393 K, together with the literature of $Mg_{0.25}Mn_{0.75}$−D powder,[19] bulk Mg−H, and Mg−D[27] (T: temperature). The hydrogenation at 393 K is not properly completed due to the limit of the maximum applied pressure of hydrogen. The values of ΔH and ΔS for hydride dissociation were calculated from middle (ΔH_M and ΔS_M), lower (ΔH_L and ΔS_L), and upper (ΔH_U and ΔS_U) edges of the sloping plateaus. The units of ΔH and ΔS are kJ mol^{-1}−$H(D)_2$ and J K^{-1} mol^{-1}−$H(D)_2$, respectively.

large cubic unit cell (a = 0.8905 nm) with a nonsimple structure.[35] From the peak position, the interplanar distance of 411 and 330 is calculated to be 0.2104 nm, which is close to $d_{Mn411\&330}$ = 0.2099 nm of bulk Mn.[35]

In the as-deposited Mg−Mn alloy films, we find for x = 0.28 and 0.45 a single broad peak at $2\theta \approx 43°$, corresponding to the 411 and 330 reflections of Mn. The $d_{Mn411\&330}$ values are evaluated to be 0.2098 nm for x = 0.28 and 0.2108 nm for x = 0.45, which are close to those for x = 0 ($d_{Mn411\&330}$ = 0.2104 nm). Taking into account the atomic radii, this result suggests that Mg hardly dissolves into Mn in the Mg_xMn_{1-x} thin films. Our previous work showed that Mg does not dissolve in Mn in the ball-milled Mg_xMn_{1-x} (x = 0.25, 0.30, and 0.40) powders either.[19] For x = 0.64, a sudden change occurs in the diffraction pattern, in which a clear peak appears at 2θ = 34.68° corresponding to the 002 reflection of Mg. The d_{Mg002} value is evaluated to be 0.2585 nm, which indicates out-of-plane contraction (d_{Mg002} = 0.2607 nm for bulk Mg[35]). The as-deposited Mg-rich Mg_xMn_{1-x} thin film is highly textured and distorted probably by in-plane tensile stress from the substrate. The synchrotron X-ray diffraction data show the diffraction peaks of both Mg and Mn in the Mg-rich compositions of x = 0.50, 0.60, and 0.75 (Figure S2a). However, even for x = 0.50, where the volume fraction of Mg is estimated to be more than half ($V_{Mg} \approx 0.65$), as shown in Figure 3, the diffraction peaks of Mg are small and broadened, which implies that Mg domains consist of fine crystallites and/or have a heavy lattice distortion. For x = 0.75, we found the lattice contraction along the c-axis of hcp Mg, agreeing well with the out-of-plane contraction observed for x = 0.64 (Figure 4).

The Mg_xMn_{1-x} thin films were hydrogenated under 3 MPa H_2 at room temperature for 12 h. For the Mn-rich composition (x = 0.28), we observe in Figure 4 that the peak corresponding to the 411 and 330 reflections of Mn slightly shifts to the lower 2θ side upon hydrogenation. The $d_{Mn411\&330}$ value increases to 0.2117 nm. We suggest that the out-of-plane expansion of Mn is induced by hydrogenation of fine Mg domains distributed in a Mn matrix, accompanying compressive stress in the MgH_2 lattice from the harder Mn matrix (Young's modulus E: E_{Mg} = 45 GPa and E_{Mn} = 198 GPa[36]). Indeed, we have found that MgD_2 domains are heavily strained in the $Mg_{0.25}Mn_{0.75}$−D powder, which contributes to the destabilization.[19] With increasing the Mg content (x = 0.45 and 0.64), peak shift of Mn upon hydrogenation becomes unclear due to peak broadening. The synchrotron X-ray diffraction data show that the unit cell volume of Mn is not affected by hydrogenation for x = 0.50, 0.60, and 0.75 (Figure S2b). These results suggest that fine and hard Mn domains are hardly deformed by hydrogenation of the Mg matrix consisting of fine crystallites (Figure S2a) because the volume expansion by hydrogenation may be relaxed at the precise grain boundaries in the $Mg(H_2)$ matrix. To obtain destabilized MgH_2, the key role is the heavy lattice distortion of MgH_2 induced by hydrogenation of embedded fine Mg in the Mn-rich compositions.

Thermodynamic Stability and Destabilization Mechanism of MgH_2 in the Mn-Rich $Mg_xMn_{1-x}-H_2$ System. The $P-T$ isotherm at 293 K indicated that MgH_2 in the $Mg_{0.30}Mn_{0.70}$−H thin film shows a higher desorption pressure of hydrogen than the samples with a higher Mg content (Figure 2). In this section, we show the temperature dependence of the hydrogen absorption/desorption property and discuss the thermodynamic nature. Figure 5a shows the $P-T$ isotherms for the $Mg_{0.30}Mn_{0.70}-H_2$ system at 293, 333, 363, and 393 K. The isotherm at 293 K is the same data shown in Figure 2. We adjusted the measurement setup and conditions to measure full absorption and desorption of hydrogen at each temperature. However, the hydrogenation at 393 K was not properly completed due to the limit of the maximum applied pressure of hydrogen, which leads to a much smaller optical change than that at other temperatures.

Focusing on the clear isotherm in the hydrogen desorption process at 333 K, we observe two sloping plateau regions [the lower region of $\ln(T/T_0) < 0.4$ and the upper one of $\ln(T/T_0) > 0.8$]. We suggest that the sloping nature of the plateaus can be explained to be due to a size distribution of the Mg domains.[16,18] Thus, a part of the Mg is not small enough to destabilize MgH_2, corresponding to the lower plateau region, which is close to the plateau pressure of $P \approx 2.4$ Pa calculated from the Van't Hoff plot for bulk MgH_2.[27]

To evaluate the thermodynamic stability of destabilized MgH_2 in the $Mg_{0.30}Mn_{0.70}$−H thin film, the Van't Hoff plots for the upper plateaus in the desorption process of hydrogen are provided, as shown in Figure 5b. The data of the

https://doi.org/10.1021/acs.inorgchem.1c02525
Inorg. Chem. 2021, 60, 15024−15030

$Mg_{0.25}Mn_{0.75}$−D powder (ΔH = 71.5 kJ mol^{-1}−D_2 and ΔS = 131.6 J K^{-1} mol^{-1}−D_2),[19] bulk Mg−H (ΔH = 74.4 kJ mol^{-1}−H_2 and ΔS = 135.1 J K^{-1} mol^{-1}−H_2), and Mg−D (ΔH = 73.1 kJ mol^{-1}−D_2 and ΔS = 135.9 J K^{-1} mol^{-1}−D_2)[27] are also shown. From middle, lower, and upper edges of the sloping plateaus at 333, 363, and 393 K, the values of ΔH and ΔS are varied from ΔH_L = 62.4 kJ mol^{-1}−H_2 and ΔS_L = 113.4 J K^{-1} mol^{-1}−H_2 to ΔH_U = 46.3 kJ mol^{-1}−H_2 and ΔS_U = 86.7 J K^{-1} mol^{-1}−H_2. This result indicates that more destabilized MgH_2 domains are formed in the thin films compared to the $Mg_{0.25}Mn_{0.75}$−D powder.[19] Moreover, we find a tendency for reduction of ΔS with decreasing ΔH. The increase in the desorption pressure of hydrogen at a given temperature is less than expected pressures due to the change in ΔS. This ΔH−ΔS relation has been observed especially in the Mg−Ti−H system.[12,14,37] Notably, Anastasopol et al. have reported ΔH = −45 kJ mol^{-1}−H_2 and ΔS = −84 J K^{-1} mol^{-1}−H_2 (for hydride formation) for Mg−Ti−H nanocomposites synthesized by spark discharge generation,[12] which are close to our result at the upper edge of the sloping plateau of the $Mg_{0.30}Mn_{0.70}$−H thin film (ΔH_U and ΔS_U). The enthalpy change is attributed to lattice distortion by nanosizing, and the entropy change is attributed to heterogeneity of the hydrogen occupation sites in the distorted lattice.[12]

It has been recognized that the immiscible combination of MgH_2/TiH_2 allows the destabilization of MgH_2 in the Mg−Ti−H system;[16,17] likewise, the destabilization of MgH_2 also in the Mg−Mn−H system has been demonstrated for the powders at 473−523 K[19,20] and the present thin films at 293−393 K. Indeed, tuning the thermodynamic stability of MgH_2 by nanosizing and facing with the immiscible metals is one of the promising ways to develop Mg-based materials for advanced hydrogen storage and supply systems. The advantage of this kind of metal hydrides is exhibited at moderate temperatures (T^{-1} = 3.3− 3.5 × 10^{-3} K^{-1}, i.e., around room temperature) where the desorption pressure of hydrogen is ∼2.5 orders of magnitude higher than that for conventional bulk Mg, as shown in Figure 5b. In other words, the operation to store and release hydrogen at lower temperatures is high in utility value since the small ΔH and ΔS enhance the elevating effect of the hydrogen desorption pressure at the given temperatures.

From the nanostructural point of view, we should again consider the operation temperature. Although both the present thin films (Figure S1) and the previous powder[19,20] could reversibly absorb and desorb hydrogen several times, they would be eventually decomposed into each metal phase by heating and aging. The exothermic heat during hydrogenation affects temperature in the reaction field. When the phase segregation and nucleation can be prevented, the lattice distortion induced by nanosizing, which is a major origin of the destabilization of MgH_2, would be relaxed by the exothermic heat. In this work, the exothermic heat during hydrogenation of Mg−Mn layers might be radiated through the Mn domains and substrate, resulting in keeping the destabilization effect. In the case of powder/bulk, the metallographic structure consisting of fine Mg domains embedded in a nonhydride-forming matrix plays a key role in keeping nanosized Mg domains and their lattice distortion. Envisioning future practical uses, our next challenge is to improve and scale up the mixing technology of Mg and immiscible metals and to optimize handling the heat transfer and radiation from the Mg domains during hydrogen uptake.

CONCLUSIONS

In the present work, we have shown the perspective that the thermodynamic stability of MgH_2 is lowered by mixing with an immiscible metal, Mn. We found that the desorption pressure of hydrogen from MgH_2 in the Mn-rich Mg−Mn alloy thin films exhibited ∼2.5 orders of magnitude increase compared to conventional bulk Mg at moderate temperatures. This destabilization phenomenon is attributed notably to heavy lattice distortion in the nanometer-sized Mg(H_2) domains, resulting in tailoring the enthalpy and entropy for hydride dissociation. The obtained thermodynamic nature to elevate the desorption pressure of hydrogen is effective at lower temperatures, which offers the potential to develop into bulk materials introduced into efficient and inexpensive hydrogen energy systems.

ASSOCIATED CONTENT

Supporting Information

The Supporting Information is available free of charge at https://pubs.acs.org/doi/10.1021/acs.inorgchem.1c02525.

Cyclic reproducibility of optical responses of the Mg_xMn_{1-x}−H_2 system and structural analysis of Mg_xMn_{1-x}(−H) thin films by synchrotron X-ray diffraction (PDF)

AUTHOR INFORMATION

Corresponding Author

Kohta Asano − *Energy Process Research Institute, National Institute of Advanced Industrial Science and Technology (AIST), Tsukuba, Ibaraki 305-8569, Japan;* orcid.org/0000-0003-4208-7303; Email: k.asano@aist.go.jp

Authors

Yanshan Lu − *Energy Process Research Institute, National Institute of Advanced Industrial Science and Technology (AIST), Tsukuba, Ibaraki 305-8569, Japan; Hydrogen Energy Research Center, Guangzhou Power Supply Bureau, Guangdong Power Grid Company Limited, Guangzhou, Guangdong 510620, China*

Herman Schreuders − *Materials for Energy Conversion and Storage, Department of Chemical Engineering, Faculty of Applied Sciences, Delft University of Technology, 2629 HZ Delft, The Netherlands*

Hyunjeong Kim − *Energy Process Research Institute, National Institute of Advanced Industrial Science and Technology (AIST), Tsukuba, Ibaraki 305-8569, Japan*

Kouji Sakaki − *Energy Process Research Institute, National Institute of Advanced Industrial Science and Technology (AIST), Tsukuba, Ibaraki 305-8569, Japan;* orcid.org/0000-0003-4781-1073

Akihiko Machida − *Synchrotron Radiation Research Center, National Institutes for Quantum and Radiological Science and Technology (QST), 679-5148 Hyogo, Japan*

Tetsu Watanuki − *Synchrotron Radiation Research Center, National Institutes for Quantum and Radiological Science and Technology (QST), 679-5148 Hyogo, Japan*

Bernard Dam − *Materials for Energy Conversion and Storage, Department of Chemical Engineering, Faculty of Applied Sciences, Delft University of Technology, 2629 HZ Delft, The Netherlands;* orcid.org/0000-0002-8584-7336

Complete contact information is available at: https://pubs.acs.org/10.1021/acs.inorgchem.1c02525

https://doi.org/10.1021/acs.inorgchem.1c02525
Inorg. Chem. 2021, 60, 15024−15030

Notes

The authors declare no competing financial interest.

■ ACKNOWLEDGMENTS

This work was supported by the International Joint Research Program for Innovative Energy Technology by the Ministry of Economy, Trade and Industry (METI) of Japan, by the Photon and Quantum Basic Research Coordinated Development Program from the Ministry of Education, Culture, Sports, Science, and Technology (MEXT) of Japan, and by Japan Society for the Promotion of Science (JSPS) Kakenhi Grant 21H01744. The synchrotron X-ray experiments were performed using the QST experimental station at the JAEA beamline of BL22XU (proposal no. 2018A3784 and 2019A3783) at SPring-8 under the Shared Use Program of JAEA and QST Facilities (proposal no. 2018A-H18 and 2019A-H17). The use of the JAEA beamline of BL22XU is also supported by the JAEA and QST Advanced Characterization Nanotechnology Platform under remit of "Nanotechnology Platform" of MEXT of Japan under proposal no. JPMXP09A18QS0016 and JPMXPA19QS0017.

■ REFERENCES

(1) The Future of Hydrogen, IEA Technology report. https://www.iea.org/reports/the-future-of-hydrogen (accessed on June 2019).
(2) US DOE. Hydrogen Strategy, Enabling A Low-Carbon Economy. https://www.energy.gov/sites/prod/files/2020/07/f76/USDOE_FE_Hydrogen_Strategy_July2020.pdf (accessed on July 2020).
(3) Rönsch, S.; Schneider, J.; Matthischke, S.; Schlüter, M.; Götz, M.; Lefebvre, J.; Prabhakaran, P.; Bajohr, S. Review on Methanation - From Fundamentals to Current Projects. *Fuel* **2016**, *166*, 276−296.
(4) Schlapbach, L.; Züttel, A. Hydrogen-storage Materials for Mobile Applications. *Nature* **2001**, *414*, 353−358.
(5) Sakintuna, B.; Lamaridarkrim, F.; Hirscher, M. Metal Hydride Materials for Solid Hydrogen Storage: A Review. *Int. J. Hydrogen Energy* **2007**, *32*, 1121−1140.
(6) Liang, J. J. Theoretical insight on tailoring energetics of Mg hydrogen absorption/desorption through nano-engineering. *Appl. Phys. A: Mater. Sci. Process.* **2005**, *80*, 173−178.
(7) Wagemans, R. W. P.; van Lenthe, J. H.; de Jongh, P. E.; van Dillen, A. J.; de Jong, K. P. Hydrogen Storage in Magnesium Clusters: Quantum Chemical Study. *J. Am. Chem. Soc.* **2005**, *127*, 16675−16680.
(8) Liu, J.; Fu, Y.; Huang, W.; Wang, H.; Ouyang, L.; Zeng, M.; Zhu, M. Direct Microstructural Evidence on the Catalyzing Mechanism for De/hydrogenation of Mg by Multi-valence NbOx. *J. Phys. Chem. C* **2020**, *124*, 6571−6579.
(9) Xin, G.; Yuan, H.; Jiang, L.; Wang, S.; Liu, X.; Li, X. Promising Gaseous and Electrochemical Hydrogen Storage Properties of Porous Mg-Pd Films Under Mild Conditions. *Phys. Chem. Chem. Phys.* **2015**, *17*, 13606−13612.
(10) Qiu, J.; Wu, F.; Jin, X.; Gu, X.; Cai, W.; Sun, D.; Fang, F. Controllable Optical Transitions of Amorphous Mg and Mg-Ni Films via Electrochemical Methods. *Phys. Chem. Chem. Phys.* **2015**, *17*, 13340−13346.
(11) Baldi, A.; Gonzalez-Silveira, M.; Palmisano, V.; Dam, B.; Griessen, R. Destabilization of the Mg-H System through Elastic Constraints. *Phys. Rev. Lett.* **2009**, *102*, 226102.
(12) Anastasopol, A.; Pfeiffer, T. V.; Middelkoop, J.; Lafont, U.; Canales-Perez, R. J.; Schmidt-Ott, A.; Mulder, F. M.; Eijt, S. W. H. Reduced Enthalpy of Metal Hydride Formation for Mg-Ti Nanocomposites Produced by Spark Discharge Generation. *J. Am. Chem. Soc.* **2013**, *135*, 7891−7900.
(13) Calizzi, M.; Venturi, F.; Ponthieu, M.; Cuevas, F.; Morandi, V.; Perkisas, T.; Bals, S.; Pasquini, L. Gas-phase synthesis of Mg-Ti nanoparticles for solid-state hydrogen storage. *Phys. Chem. Chem. Phys.* **2016**, *18*, 141−148.
(14) Patelli, N.; Calizzi, M.; Migliori, A.; Morandi, V.; Pasquini, L. Hydrogen Desorption Below 150 °C in MgH_2-TiH_2 Composite Nanoparticles: Equilibrium and Kinetic Properties. *J. Phys. Chem. C* **2017**, *121*, 11166−11177.
(15) Mooij, L. P. A.; Baldi, A.; Boelsma, C.; Shen, K.; Wagemaker, M.; Pivak, Y.; Schreuders, H.; Griessen, R.; Dam, B. Interface Energy Controlled Thermodynamics of Nanoscale Metal Hydrides. *Adv. Energy Mater.* **2011**, *1*, 754−758.
(16) Asano, K.; Westerwaal, R. J.; Anastasopol, A.; Mooij, L. P. A.; Boelsma, C.; Ngene, P.; Schreuders, H.; Eijt, S. W. H.; Dam, B. Destabilization of Mg Hydride by Self-Organized Nanoclusters in the Immiscible Mg-Ti System. *J. Phys. Chem. C* **2015**, *119*, 12157−12164.
(17) Asano, K.; Kim, H.; Sakaki, K.; Jimura, K.; Hayashi, S.; Nakamura, Y.; Ikeda, K.; Otomo, T.; Machida, A.; Watanuki, T. Structural Variation of Self-Organized Mg Hydride Nanoclusters in Immiscible Ti Matrix by Hydrogenation. *Inorg. Chem.* **2018**, *57*, 11831−11838.
(18) Asano, K.; Westerwaal, R. J.; Schreuders, H.; Dam, B. Enhancement of Destabilization and Reactivity of Mg Hydride Embedded in Immiscible Ti Matrix by Addition of Cr: Pd-Free Destabilized Mg Hydride. *J. Phys. Chem. C* **2017**, *121*, 12631−12635.
(19) Lu, Y.; Kim, H.; Sakaki, K.; Hayashi, S.; Jimura, K.; Asano, K. Destabilizing the Dehydrogenation Thermodynamics of Magnesium Hydride by Utilizing the Immiscibility of Mn with Mg. *Inorg. Chem.* **2019**, *58*, 14600−14607.
(20) Lu, Y.; Kim, H.; Jimura, K.; Hayashi, S.; Sakaki, K.; Asano, K. Strategy of Thermodynamic and Kinetic Improvements for Mg Hydride Nanostructured by Immiscible Transition Metals. *J. Power Sources* **2021**, *494*, 229742.
(21) Guzik, M. N.; Deledda, S.; Sørby, M. H.; Yartys, V. A.; Hauback, B. C. New FCC Mg-Zr and Mg-Zr-Ti Deuterides Obtained by Reactive Milling. *J. Solid State Chem.* **2015**, *226*, 237−242.
(22) Bao, S.; Yamada, Y.; Tajima, K.; Jin, P.; Okada, M.; Yoshimura, K. Switchable Mirror Based on Mg-Zr-H Thin Films. *J. Alloys Compd.* **2012**, *513*, 495−498.
(23) Bystrzycki, J.; Czujko, T.; Varin, R. A. Processing by Controlled Mechanical Milling of Nanocomposite Powders Mg + X (X = Co, Cr, Mo, V, Y, Zr) and Their Hydrogenation Properties. *J. Alloys Compd.* **2005**, *404*−*406*, 507−510.
(24) Liang, G.; Huot, J.; Boily, S.; Van Neste, A.; Schulz, R. Catalytic Effect of Transition Metals on Hydrogen Sorption in Nanocrystalline Ball Milled MgH_2-Tm (Tm=Ti, V, Mn, Fe and Ni) Systems. *J. Alloys Compd.* **1999**, *292*, 247−252.
(25) Kalisvaart, W. P.; Harrower, C. T.; Haagsma, J.; Zahiri, B.; Luber, E. J.; Ophus, C.; Poirier, E.; Fritzsche, H.; Mitlin, D. Hydrogen Storage in Binary and Ternary Mg-based Alloys: A Comprehensive Experimental Study. *Int. J. Hydrogen Energy* **2010**, *35*, 2091−2103.
(26) Edalati, K.; Emami, H.; Staykov, A.; Smith, D. J.; Akiba, E.; Horita, Z. Formation of Metastable Phases in Magnesium-Titanium System by High-pressure Torsion and Their Hydrogen Storage Performance. *Acta Mater.* **2015**, *99*, 150−156.
(27) Stampfer, J. F.; Holley, C. E.; Suttle, J. F. The Magnesium-Hydrogen System1-3. *J. Am. Chem. Soc.* **1960**, *82*, 3504−3508.
(28) Gremaud, R.; Broedersz, C. P.; Borsa, D. M.; Borgschulte, A.; Mauron, P.; Schreuders, H.; Rector, J. H.; Dam, B.; Griessen, R. Hydrogenography: An Optical Combinatorial Method to Find New Light-Weight Hydrogen-Storage Materials. *Adv. Mater.* **2007**, *19*, 2813−2817.
(29) Gremaud, R.; Slaman, M.; Schreuders, H.; Dam, B.; Griessen, R. An Optical Method to Determine the Thermodynamics of Hydrogen Absorption and Desorption in Metals. *Appl. Phys. Lett.* **2007**, *91*, 231916.
(30) Watanuki, T.; Machida, A.; Ikeda, T.; Ohmura, A.; Kaneko, H.; Aoki, K.; Sato, T. J.; Tsai, A. P. Development of a Single-Crystal X-ray Diffraction System for Hydrostatic-Pressure and Low-Temperature Structural Measurement and Its Application to the Phase Study of Quasicrystals. *Philos. Mag.* **2007**, *87*, 2905−2911.

https://doi.org/10.1021/acs.inorgchem.1c02525
Inorg. Chem. 2021, 60, 15024−15030

(31) Kim, H.; Schreuders, H.; Sakaki, K.; Asano, K.; Nakamura, Y.; Maejima, N.; Machida, A.; Watanuki, T.; Dam, B. Unveiling Nanoscale Compositional and Structural Heterogeneities of Highly Textured $Mg_{0.7}Ti_{0.3}Hy$ Thin Films. *Inorg. Chem.* **2020**, *59*, 6800−6807.
(32) *Phase Diagrams of Binary Hydrogen Alloys*; Manchester, F. D., Ed.; ASM International: Materials Park, OH, 2000.
(33) Griessen, R. Science and Technology of Hydrogen in Metals. 2003, http://www.nat.vu.nl/griessen/ (accessed September 17, 2021).
(34) Baldi, A.; Mooij, L.; Palmisano, V.; Schreuders, H.; Krishnan, G.; Kooi, B. J.; Dam, B.; Griessen, R. Elastic versus Alloying Effects in Mg-Based Hydride Films. *Phys. Rev. Lett.* **2018**, *121*, 255503.
(35) MatNavi. NIMS Materials Database, 2018. http://mits.nims.go.jp/index_en.html.
(36) *Metal Databook Ver. 3*. Japan Institute of Metals, 1993.
(37) Mulder, F. M.; Singh, S.; Bolhuis, S.; Eijt, S. W. H. Extended Solubility Limits and Nanograin Refinement in Ti/Zr Fluoride-Catalyzed MgH_2. *J. Phys. Chem. C* **2012**, *116*, 2001−2012.

https://doi.org/10.1021/acs.inorgchem.1c02525
Inorg. Chem. 2021, 60, 15024−15030